Odor coding in the olfactory bulb

Takeshi Imai[1]*
[1]1Graduate School of Medical Sciences, Kyushu University, Fukuoka, Japan
*Corresponding author. Tel: +81-92-642-6086; Fax: +81-92-642-6094
E-mail address: t-imai@med.kyushu-u.ac.jp

Keywords: combinatorial receptor code; olfactory bulb; glomerulus; odor map; mitral/tufted cells; short axon cells; granule cells; mechanosensation; temporal coding; theta oscillations; phase coding; concentration invariance; plasticity; piriform cortex

Synopsis

Odor signals that are detected by olfactory sensory neurons are represented as an odor map in their axon terminals in the olfactory bulb. In the mitral/tufted cells of the olfactory bulb, odor information is represented not only by the firing rate, but also by the temporal patterns of activity (phase coding), which is utilized for concentration-invariant odor identity coding. Mitral/tufted cell activity also shows plastic changes to efficiently and robustly recognize odors in a context-dependent manner.

Abstract

The olfactory system detects and discriminates a huge variety of airborne odorants. These odor signals can then be used to induce stereotyped behaviors, such as attraction and aversion, or can be used in learning to make more flexible behavioral decisions. A remarkable feature of the olfactory system is its ability to recognize the odor identities irrespective of their concentrations and sniffing conditions. Toward these difficult tasks in olfaction, odor signals are strategically represented as spatiotemporal patterns of activity in the olfactory bulb. In this chapter, I describe how odor information is processed and represented within the olfactory bulb, with a particular focus on the temporal patterns of activity. I then discuss how these temporal patterns are utilized for concentration-invariant odor perception.

1. Combinatorial receptor code in the olfactory sensory neurons

Airborne odorants are detected by odorant receptors (ORs) expressed in olfactory sensory neurons (OSNs). There are ~1,000 functional ORs in mice, and ~390 functional ORs in humans. In contrast, there is an extremely high variability in the type of odorants detected. The putative number of odorants detectable by human is thought to be within the order of many thousands. In addition, animals can discriminate between different combinations of chemicals. Therefore, the coding capacity of the mammalian olfactory system is extremely large.

If each OR detects just one odorant, the olfactory system could cover only ~1,000 chemicals. How can the olfactory system handle such a large number of chemicals with a limited number of ORs? It has been shown that each OSN exclusively expresses one type of OR out of the large repertoire, but it can still detect multiple chemical species. Similarly, each chemical is typically detected by multiple types of ORs, namely the combination of ~1,000 ORs. This "combinatorial receptor code" is the basis for the large discriminatory capacity at the level of OSNs (Malnic et al., 1999; Saito et al., 2009). It is also suggested that some odorants act as antagonists, further tuning the representation of odor mixtures already at the level of OSNs (Oka et al., 2004).

It should be noted, however, that some odorants are detected by one or a few ORs. The activation or inactivation of a single type of OSNs can change odor perception in such cases (Keller et al., 2007; Dewan et al., 2013; Smear et al., 2013; Shirasu et al., 2014).

2. Odor map and domain organization in the olfactory bulb

OSNs send odor information to the glomeruli in the olfactory bulb (OB). How is the odor information represented in the glomerular layer of the OB? While OSNs expressing a given type of OR are scattered in the olfactory epithelium, their axons converge onto a few glomeruli in the olfactory bulb. As a result, the activation patterns of ORs are represented by ~1,000 sets of glomeruli in the OB. Using intrinsic imaging, calcium imaging, and 2-deoxyglucose radiography, it has been suggested that similar odors tend to activate glomeruli in a similar area in the OB (Rubin and Katz, 1999; Johnson and Leon, 2000; Uchida et al., 2000; Wachowiak and Cohen, 2001). As a result, at a global level, there seems to be a chemotopic representation. It has been reported that response areas for some odorants are well correlated with the genetically-defined OB domains for different classes of ORs. For example, aliphatic acids tend to activate D_I domains, whereas ketones and aromatic compounds tend to activate D_{II} domains (Kobayakawa et al., 2007; Bozza et al., 2009) (Figure 1). Some amines

activate D_{III} domains, which receive projections from OSNs expressing the TAAR-family of ORs (Pacifico et al., 2012). Based on molecular receptive range of the glomerulus, the OB can be separated into several clusters (Mori et al., 2006). However, chemotopy is not evident at a local scale: in other words, similar odors do not necessarily activate neighboring glomeruli (Ma et al., 2012).

Currently we do not know the functional roles of the cluster or domain organization. In one scenario, mitral/tufted (M/T) cells with similar molecular receptive range may be interconnected by a lateral inhibition circuit (Yokoi et al., 1995). It is also postulated that the domain organization is linked to specific innate behaviors. For example, genetic ablation experiments demonstrated that the dorsal (D) domain of the OB mediates innate aversive responses to odorants (Kobayakawa et al., 2007). While a fox-derived smell, trimethylthiazoline (TMT) activates glomeruli in both the D and ventral (V) domains, only the D domain is involved in mediating the freezing response of mice.

3. Gain control

In the OB, inputs from OSNs are relayed to two types of excitatory neurons, mitral cells and tufted cells (M/T cells) (Figure 2A). Tufted cells receive direct synaptic inputs from OSNs, but mitral cells receive more indirect and processed inputs via external tufted cells (De Saint Jan et al., 2009; Gire et al., 2012). In addition, various types of interneurons tune the sensory inputs. GABAergic periglomerular cells act not only on M/T cells, but also on OSN axon terminals, which is a form of pre-synaptic inhibition (Murphy et al., 2005; Wachowiak et al., 2005). These inhibitory inputs act as an intraglomerular gain control mechanism (Figure 2B). More global forms of gain control are mediated by other types of interneurons: parvalbumin-expressing interneurons (PV neurons) in the external plexiform layer (Kato et al., 2013; Miyamichi et al., 2013), and short axon cells expressing the dopamine transporter (DAT) (Banerjee et al., 2015) (Figure 2B). These interneurons send dense and widespread inhibitions back to M/T cells, thereby controlling the gain at a global level. Many of these interneurons form reciprocal synapses. As a result of these gain control mechanisms, M/T cell responses are more consistent across the odor concentrations than in the OSNs (Storace and Cohen, 2017). This is one of the mechanisms for concentration-invariant odor perception (Uchida et al., 2013).

4. Lateral inhibition

In addition to the global inhibition, lateral inhibition tunes the odor responses in M/T cells (Yokoi et al., 1995). In the OB, there seem to be two different types of lateral

inhibition. In the first stage, GABAergic and dopaminergic short axon cells mediate interglomerular lateral inhibition (Kosaka and Kosaka, 2008; Kiyokage et al., 2010; Whitesell et al., 2013) (Figure 2C). At this stage, the glomerulus is a functional unit for the lateral inhibition. The interglomerular lateral inhibition by short axon cells are sparse, selective, and long range (Whitesell et al., 2013; Economo et al., 2016).

While M/T cells associated with a common glomerulus (known as sister M/T cells) receive shared synaptic inputs and are electrically coupled via gap junctions within the glomerulus (Schoppa and Westbrook, 2001; Christie et al., 2005; Hayar et al., 2005), their somata are spatially scattered (Ke et al., 2013; Kikuta et al., 2013). The second level of lateral inhibition is thought to occur among individual M/T cells which is mediated by granule cells (Yokoi et al., 1995) (Figure 2C). Granule cells mainly target the lateral dendrites and somata of M/T cells. Lateral dendrites extend up to 1 mm in length and their patterns are variable even among sister M/T cells (Ke et al., 2013). As a result, odor response tuning is different even among sister M/T cells (Dhawale et al., 2010; Kikuta et al., 2013), which suggests that sister M/T cells are non-redundant in odor coding. Trans-synaptic virus tracing experiments suggest that lateral inhibition by granule cells are also sparse and selective (Kim et al., 2011).

Thus, odor signals are transformed non-linearly, firstly between OSNs and M/T cell primary dendrites, and then between primary dendrite inputs and M/T cell outputs (somata). These sparse and selective lateral inhibitions are different from the dense center-surround inhibition known in other sensory systems (e.g., the retina), where sensory stimuli are represented in a continuous manner. It remains poorly understood how the lateral inhibition helps the odor coding in the non-continuous odor map.

5. Temporal representation of odor information in M/T cells

Rodents inhale odorants by sniffing at 2-10 Hz range (Kepecs et al., 2007). Furthermore, rodents can discriminate odors within a single sniff (Uchida and Mainen, 2003). This indicates that each sniff is a minimum unit (packet) for odor information processing (Kepecs et al., 2006). Odor stimuli change not only the firing rate, but also temporal patterns of firing in M/T cells. Electrophysiological and voltage imaging studies in anesthetized and awake animals have demonstrated that odor produces rich temporal patterns of activity coupled to the sniff cycles (Macrides and Chorover, 1972; Spors and Grinvald, 2002; Margrie and Schaefer, 2003; Bathellier et al., 2008; Cury and Uchida, 2010; Shusterman et al., 2011).

M/T cells show sniff coupled oscillatory activity without odors (Adrian, 1942). Upon olfactory stimulation, M/T cells show bursting activity at specific times within a

sniff cycle, which are highly consistent across sniffs. The activation timing is more consistent within the relative time (sniff phase) than the absolute time, and can be explained by the fluid dynamics of the inhaled odorous air (Shusterman et al., 2011; Shusterman et al., 2018). The odor-evoked activation phase is unique to each odor and M/T cells (Shusterman et al., 2011), suggesting that phase information can be utilized in olfactory coding (phase coding) (Kepecs et al., 2006) (Figure 3A, B).

This possibility was directly tested by using the optogenetic activation of a single glomerulus (M72-ChR2 glomerulus). After the training, mice were able to discriminate between different activation timings within each sniff for the glomerulus (Smear et al., 2013) (Figure 3C). These results suggest that the activation phase can be utilized for odor discrimination.

6. Mechanosensory-based oscillations in M/T cells

The sniff-coupled oscillatory activity (also known as theta oscillations) in M/T cells is driven by OSNs, rather than by centrifugal inputs. OSNs robustly respond to mechanical stimuli produced by the nasal airflow (Grosmaitre et al., 2007; Chen et al., 2012; Iwata et al., 2017) (Figure 4A). This means that OSNs are dual-modal sensors, detecting both odors and mechanical signals. The mechanosensitivity of OSNs is determined by the expressed OR, suggesting that ORs are involved in mechanosensation, directly or indirectly (Connelly et al., 2015). These sniff-coupled mechanosensory signals are used to produce the oscillatory activities seen in M/T cells. The oscillation phases are heterogeneous and unique to each glomerulus (Figure 4B), but are stable across different sniff speeds and frequencies (Iwata et al., 2017). In contrast, it is the odor stimuli that produce the odor-specific activation phase. Therefore, this phase coding strategy can distinguish odor vs. mechanical stimuli, even though they are both coming from OSNs (Iwata et al., 2017) (Figure 4C-E). Thus, mechanosensation in OSNs does not mask odor detection. Rather, mechanosensory-based oscillations facilitate the temporally precise phase coding in M/T cells, this is particularly useful for odors at a low concentration which would otherwise produce unreliable responses (Iwata et al., 2017).

7. Concentration invariant phase coding

Another remarkable feature of the phase coding is concentration invariance. As the odor concentration increases, more OSNs will be activated. While the gain control can help some, this still happens for M/T cells. Moreover, the odor map pattern is dynamically rearranged as the concentration changes (Figure 5A, left). Nevertheless, animals can

easily tell the identity of an odor irrespective of the odor concentration. For example, animals can identify and track the increasing concentrations of an odor to find their food. The neural basis for the concentration invariant odor perception has been a long-standing question in the field.

Recent studies indicate that the phase coding in M/T cells is the key for the concentration-invariant odor identity coding. While the firing rate (rate code) of M/T cells dynamically changes as the odor concentration increases, the phase code is stable across different concentrations (Margrie and Schaefer, 2003; Iwata et al., 2017) (Figure 5A, right). Furthermore, the phase code can better discriminate identities of two different odors with variable concentrations. Therefore, phase coding in M/T cells may be the basis for the concentration-invariant odor identity coding (Figure 5A, bottom). The rate code may be a good candidate for the odor intensity coding. Similar phase coding systems are also known to occur in place cells in hippocampus, and whisker system in rodents (Huxter et al., 2003; Kleinfeld and Deschenes, 2011; Severson et al., 2017).

Currently the circuit mechanisms for the phase coding remain unknown. Earlier studies indicated that subthreshold oscillations may be the key, but recent results are more complicated than as previously predicted (Hopfield, 1995; Margrie and Schaefer, 2003). As phase coding is not evident in OSN somata (Iwata et al., 2017), OB circuitry may play a major role. Mechanosensory inputs from OSNs and periglomerular interneurons seem to be key players (Fukunaga et al., 2014; Iwata et al., 2017).

While accumulating evidence shows the importance of the phase coding in the main olfactory bulb, we do not argue that all the odorants are encoded in that way. For example, some of the highly selective pheromones or kairomones may be encoded solely by rate coding. In fact, the sniff-based fine temporal patterns are absent in the accessory olfactory bulb, and the phase coding scheme is unlikely (Yoles-Frenkel et al., 2018). In addition, different cortical areas may have different decoding strategies.

8. Decoding concentration-invariant phase code in the piriform cortex

M/T cells send out odor information to the olfactory cortex, among which, the piriform cortex is the largest area, and it plays a major role in olfactory learning. In the piriform cortex, fine temporal patterns are not evident. Odor signals are represented by different ensembles of neurons based on rate coding, which is concentration invariant (Stettler and Axel, 2009; Miura et al., 2012; Bolding and Franks, 2018). These results suggest that the phase code in M/T cells are transformed to the rate code in the piriform cortex.

Neurons in the piriform cortex receive convergent inputs from multiple M/T cells

directly or indirectly (Arenkiel et al., 2007; Apicella et al., 2010; Miyamichi et al., 2011). Furthermore, the activation of these neurons is input timing-dependent. For example, when glomerulus A and B are activated in a different temporal sequence, different sets of piriform neurons will be activated (Haddad et al., 2013). This is in part, ensured by the global recurrent network within the piriform cortex (Bolding and Franks, 2018). When the recurrent network is inactivated, odor responses in the piriform cortex become concentration-dependent (Figure 5B). As a result, odor identity discrimination across different concentrations becomes more difficult when analyzed with a linear decoder (Figure 5C). These results suggest that the global feedback inhibition within the piriform cortex is important to produce the concentration invariant responses seen. Some studies propose that M/T cell activation at an earlier sniff phase may be more important signatures for the odor identity coding (Wilson et al., 2017; Bolding and Franks, 2018), but others do not support this notion (Cury and Uchida, 2010; Haddad et al., 2013; Iwata et al., 2017). This issue needs to be further investigated in future studies.

9. Plasticity in M/T cell responses

Odor representation in M/T cells is heavily tuned by the brain state. Compared to the anesthetized state, in awake animals the odor responses of M/T cells are sparser and smaller in M/T cells, in part due to the elevated granule cell activity (Kato et al., 2012). Furthermore, odor-evoked responses at a time scale of several seconds are more dynamic in the awake state. This helps with the decorrelation of M/T cell responses to similar odorants (Niessing and Friedrich, 2010; Kato et al., 2012), which is mediated by cortical feedback (Otazu et al., 2015). Neuromodulators, including acetylcholine, noradrenaline, and serotonin, also tune odor responses in M/T cells (Fletcher and Chen, 2010). For example, cholinergic inputs from the basal forebrain sharpen the odor responses of M/T cells and help odor discrimination behavior (Castillo et al., 1999; Ma and Luo, 2012; Nunez-Parra et al., 2013; Rothermel et al., 2014).

Odor representations in M/T cells are also dynamically tuned by learning. While odor representation in OSN axons is stable across several days of olfactory discrimination tasks (Chu et al., 2017), the activity of M/T cells changes dynamically. In passive odor experiences, the responses to the presented odors gradually declined (Kato et al., 2012). While mice perform difficult odor discrimination tasks with very similar odorants, the initially overlapping representation of odors gradually becomes separated to produce more reliable discrimination, this is known as pattern separation (Doucette and Restrepo, 2008; Chu et al., 2016; Yamada et al., 2017; Koldaeva et al., 2019). This

context-dependent pattern separation may be the result of cortical feedback regulation (Yamada et al., 2017). Similar plasticity seems to occur with sub-sniff temporal patterns in M/T cells (Gschwend et al., 2015).

10. Concluding remarks

The odor information detected in OSNs is firstly sorted out to ~1,000 sets of glomeruli in the OB, known as the odor map. This odor map is useful for odor tuning based on the glomerular microcircuit. The odor map is then redistributed to M/T cells for further processing. The OB is more than just a relay, performing gain control, lateral inhibition, phase coding, and learning.

In this chapter, I have also overviewed the odor coding strategy at different stages in the olfactory system, namely OSNs, M/T cells, and cortical neurons (piriform cortex). In OSNs, both mechanical and odor signals are represented by the rate code. In M/T cells, however, the mechanosensory and odor signals are separated based on phase coding. Furthermore, the phase codes, but not rate codes, are concentration-invariant. The phase code in M/T cells is then transformed into the concentration-invariant rate codes of the piriform cortex. Thus, a major function of the OB is to encode odor identity information into a robust phase code insensitive to the ever-fluctuating responses in OSNs. This phase code is then used to decode the odor identity in the piriform cortex (Figure 6).

Another remarkable feature of the OB is context-dependent plasticity. While odor responses in OSNs are relatively stable, M/T cell responses are far more dynamic and plastic. With massive cortical inputs, M/T cell responses are fine-tuned for efficient but reliable odor discrimination in awake animals.

Acknowledgement

This work was supported by a grant from the programs Grants-in-Aid for Scientific Research on Innovative Areas 'Dynamic regulation of Brain Function by Scrap & Build System' (JP16H06456 to TI) from MEXT, JSPS KAKENHI (JP17H06261, JP16K14568, JP15H05572, and JP15K14336 to TI; JP17K14946 to MNL), Brain Science Foundation (to TI). I thank M.N. Leiwe for the critical reading of this manuscript.

References

Adrian ED (1942) Olfactory reactions in the brain of the hedgehog. Journal of Physiology-London 100:459-473.

Apicella A, Yuan Q, Scanziani M, Isaacson JS (2010) Pyramidal cells in piriform cortex receive convergent input from distinct olfactory bulb glomeruli. Journal of neuroscience 30:14255-14260.

Arenkiel BR, Peca J, Davison IG, Feliciano C, Deisseroth K, Augustine GJ, Ehlers MD, Feng G (2007) In vivo light-induced activation of neural circuitry in transgenic mice expressing channelrhodopsin-2. Neuron 54:205-218.

Banerjee A, Marbach F, Anselmi F, Koh MS, Davis MB, da Silva PG, Delevich K, Oyibo HK, Gupta P, Li B, Albeanu DF (2015) An Interglomerular Circuit Gates Glomerular Output and Implements Gain Control in the Mouse Olfactory Bulb. Neuron 87:193-207.

Bathellier B, Buhl DL, Accolla R, Carleton A (2008) Dynamic ensemble odor coding in the mammalian olfactory bulb: Sensory information at different timescales. Neuron 57:586-598.

Bolding KA, Franks KM (2018) Recurrent cortical circuits implement concentration-invariant odor coding. Science 361:1088-+.

Bozza T, Vassalli A, Fuss S, Zhang JJ, Weiland B, Pacifico R, Feinstein P, Mombaerts P (2009) Mapping of Class I and Class II Odorant Receptors to Glomerular Domains by Two Distinct Types of Olfactory Sensory Neurons in the Mouse. Neuron 61:220-233.

Castillo PE, Carleton A, Vincent JD, Lledo PM (1999) Multiple and opposing roles of cholinergic transmission in the main olfactory bulb. Journal of neuroscience 19:9180-9191.

Chen XM, Xia ZG, Storm DR (2012) Stimulation of Electro-Olfactogram Responses in the Main Olfactory Epithelia by Airflow Depends on the Type 3 Adenylyl Cyclase. Journal of Neuroscience 32:15769-15778.

Christie JM, Bark C, Hormuzdi SG, Helbig I, Monyer H, Westbrook GL (2005) Connexin36 mediates spike synchrony in olfactory bulb glomeruli. Neuron 46:761-772.

Chu MW, Li WL, Komiyama T (2016) Balancing the Robustness and Efficiency of Odor Representations during Learning. Neuron 92:174-186.

Chu MW, Li WKL, Komiyama T (2017) Lack of Pattern Separation in Sensory Inputs to the Olfactory Bulb during Perceptual Learning. eNeuro 4.

Connelly T, Yu YQ, Grosmaitre X, Wang J, Santarelli LC, Savigner A, Qiao X, Wang ZS, Storm DR, Ma MH (2015) G protein-coupled odorant receptors underlie mechanosensitivity in mammalian olfactory sensory neurons. Proceedings of the National Academy of Sciences of the United States of America 112:590-595.

Cury KM, Uchida N (2010) Robust odor coding via inhalation-coupled transient activity in the mammalian olfactory bulb. Neuron 68:570-585.

De Saint Jan D, Hirnet D, Westbrook GL, Charpak S (2009) External tufted cells drive the output of olfactory bulb glomeruli. Journal of neuroscience 29:2043-2052.

Dewan A, Pacifico R, Zhan R, Rinberg D, Bozza T (2013) Non-redundant coding of aversive odours in the main olfactory pathway. Nature 497:486-+.

Dhawale AK, Hagiwara A, Bhalla US, Murthy VN, Albeanu DF (2010) Non-redundant odor coding by sister mitral cells revealed by light addressable glomeruli in the mouse. Nat neurosci 13:1404-1412.

Doucette W, Restrepo D (2008) Profound Context-Dependent Plasticity of Mitral Cell Responses in Olfactory Bulb. Plos Biology 6:2266-2285.

Economo MN, Hansen KR, Wachowiak M (2016) Control of Mitral/Tufted Cell Output by Selective Inhibition among Olfactory Bulb Glomeruli. Neuron 91:397-411.

Fletcher ML, Chen WR (2010) Neural correlates of olfactory learning: Critical role of centrifugal neuromodulation. Learn Mem 17:561-570.

Fukunaga I, Herb JT, Kollo M, Boyden ES, Schaefer AT (2014) Independent control of gamma and theta activity by distinct interneuron networks in the olfactory bulb. Nature Neuroscience 17:1208-1216.

Gire DH, Franks KM, Zak JD, Tanaka KF, Whitesell JD, Mulligan AA, Hen R, Schoppa NE (2012) Mitral cells in the olfactory bulb are mainly excited through a multistep signaling path. Journal of neuroscience 32:2964-2975.

Grosmaitre X, Santarelli LC, Tan J, Luo M, Ma M (2007) Dual functions of mammalian olfactory sensory neurons as odor detectors and mechanical sensors. Nature neuroscience 10:348-354.

Gschwend O, Abraham NM, Lagier S, Begnaud F, Rodriguez I, Carleton A (2015) Neuronal pattern separation in the olfactory bulb improves odor discrimination learning. Nature Neuroscience 18:1474-+.

Haddad R, Lanjuin A, Madisen L, Zeng HK, Murthy VN, Uchida N (2013) Olfactory cortical neurons read out a relative time code in the olfactory bulb. Nature Neuroscience 16:949-U227.

Hayar A, Shipley MT, Ennis M (2005) Olfactory bulb external tufted cells are synchronized by multiple intraglomerular mechanisms. Journal of neuroscience

25:8197-8208.
Hopfield JJ (1995) Pattern-Recognition Computation Using Action-Potential Timing for Stimulus Representation. Nature 376:33-36.
Huxter J, Burgess N, O'Keefe J (2003) Independent rate and temporal coding in hippocampal pyramidal cells. Nature 425:828-832.
Iwata R, Kiyonari H, Imai T (2017) Mechanosensory-Based Phase Coding of Odor Identity in the Olfactory Bulb. Neuron 96:1139-+.
Johnson BA, Leon M (2000) Modular representations of odorants in the glomerular layer of the rat olfactory bulb and the effects of stimulus concentration. Journal of Comparative Neurology 422:496-509.
Kato HK, Chu MW, Isaacson JS, Komiyama T (2012) Dynamic sensory representations in the olfactory bulb: modulation by wakefulness and experience. Neuron 76:962-975.
Kato HK, Gillet SN, Peters AJ, Isaacson JS, Komiyama T (2013) Parvalbumin-expressing interneurons linearly control olfactory bulb output. Neuron 80:1218-1231.
Ke MT, Fujimoto S, Imai T (2013) SeeDB: a simple and morphology-preserving optical clearing agent for neuronal circuit reconstruction. Nat Neurosci 16:1154-1161.
Keller A, Zhuang HY, Chi QY, Vosshall LB, Matsunami H (2007) Genetic variation in a human odorant receptor alters odour perception. Nature 449:468-U466.
Kepecs A, Uchida N, Mainen ZF (2006) The sniff as a unit of olfactory processing. Chemical Senses 31:167-179.
Kepecs A, Uchida N, Mainen ZF (2007) Rapid and precise control of sniffing during olfactory discrimination in rats. J Neurophysiol 98:205-213.
Kikuta S, Fletcher ML, Homma R, Yamasoba T, Nagayama S (2013) Odorant response properties of individual neurons in an olfactory glomerular module. Neuron 77:1122-1135.
Kim DH, Phillips ME, Chang AY, Patel HK, Nguyen KT, Willhite DC (2011) Lateral Connectivity in the Olfactory Bulb is Sparse and Segregated. Frontiers in Neural Circuits 5:5.
Kiyokage E, Pan YZ, Shao Z, Kobayashi K, Szabo G, Yanagawa Y, Obata K, Okano H, Toida K, Puche AC, Shipley MT (2010) Molecular identity of periglomerular and short axon cells. Journal of neuroscience 30:1185-1196.
Kleinfeld D, Deschenes M (2011) Neuronal Basis for Object Location in the Vibrissa Scanning Sensorimotor System. Neuron 72:455-468.
Kobayakawa K, Kobayakawa R, Matsumoto H, Oka Y, Imai T, Ikawa M, Okabe M,

Ikeda T, Itohara S, Kikusui T, Mori K, Sakano H (2007) Innate versus learned odour processing in the mouse olfactory bulb. Nature 450:503-508.

Koldaeva A, Schaefer AT, Fukunaga I (2019) Rapid task-dependent tuning of the mouse olfactory bulb. Elife 8.

Kosaka T, Kosaka K (2008) Tyrosine hydroxylase-positive GABAergic juxtaglomerular neurons are the main source of the interglomerular connections in the mouse main olfactory bulb. Neurosci Res 60:349-354.

Ma L, Qiu Q, Gradwohl S, Scott A, Yu EQ, Alexander R, Wiegraebe W, Yu CR (2012) Distributed representation of chemical features and tunotopic organization of glomeruli in the mouse olfactory bulb. Proceedings of the National Academy of Sciences of the United States of America 109:5481-5486.

Ma M, Luo M (2012) Optogenetic activation of basal forebrain cholinergic neurons modulates neuronal excitability and sensory responses in the main olfactory bulb. Journal of neuroscience 32:10105-10116.

Macrides F, Chorover SL (1972) Olfactory Bulb Units - Activity Correlated with Inhalation Cycles and Odor Quality. Science 175:84-&.

Malnic B, Hirono J, Sato T, Buck LB (1999) Combinatorial receptor codes for odors. Cell 96:713-723.

Margrie TW, Schaefer AT (2003) Theta oscillation coupled spike latencies yield computational vigour in a mammalian sensory system. Journal of Physiology-London 546:363-374.

Miura K, Mainen ZF, Uchida N (2012) Odor representations in olfactory cortex: distributed rate coding and decorrelated population activity. Neuron 74:1087-1098.

Miyamichi K, Shlomai-Fuchs Y, Shu M, Weissbourd BC, Luo L, Mizrahi A (2013) Dissecting local circuits: parvalbumin interneurons underlie broad feedback control of olfactory bulb output. Neuron 80:1232-1245.

Miyamichi K, Amat F, Moussavi F, Wang C, Wickersham I, Wall NR, Taniguchi H, Tasic B, Huang ZJ, He ZG, Callaway EM, Horowitz MA, Luo LQ (2011) Cortical representations of olfactory input by trans-synaptic tracing. Nature 472:191-196.

Mori K, Takahashi YK, Igarashi KM, Yamaguchi M (2006) Maps of odorant molecular features in the Mammalian olfactory bulb. Physiological Reviews 86:409-433.

Murphy GJ, Darcy DP, Isaacson JS (2005) Intraglomerular inhibition: signaling mechanisms of an olfactory microcircuit. Nat neurosci 8:354-364.

Niessing J, Friedrich RW (2010) Olfactory pattern classification by discrete neuronal

network states. Nature 465:47-U53.
Nunez-Parra A, Maurer RK, Krahe K, Smith RS, Araneda RC (2013) Disruption of centrifugal inhibition to olfactory bulb granule cells impairs olfactory discrimination. Proceedings of the National Academy of Sciences of the United States of America 110:14777-14782.
Oka Y, Omura M, Kataoka H, Touhara K (2004) Olfactory receptor antagonism between odorants. Embo Journal 23:120-126.
Otazu GH, Chae HG, Albeanu DF (2015) Cortical feedback decorrelates olfactory bulb output in awake mice. Chemical Senses 40:613-613.
Pacifico R, Dewan A, Cawley D, Guo CY, Bozza T (2012) An Olfactory Subsystem that Mediates High-Sensitivity Detection of Volatile Amines. Cell Rep 2:76-88.
Rothermel M, Carey RM, Puche A, Shipley MT, Wachowiak M (2014) Cholinergic inputs from Basal forebrain add an excitatory bias to odor coding in the olfactory bulb. The Journal of neuroscience : the official journal of the Society for Neuroscience 34:4654-4664.
Rubin BD, Katz LC (1999) Optical imaging of odorant representations in the mammalian olfactory bulb. Neuron 23:499-511.
Saito H, Chi QY, Zhuang HY, Matsunami H, Mainland JD (2009) Odor Coding by a Mammalian Receptor Repertoire. Sci Signal 2.
Sakaguchi R, Leiwe MN, Imai T (2018) Bright multicolor labeling of neuronal circuits with fluorescent proteins and chemical tags. Elife 7.
Schoppa NE, Westbrook GL (2001) Glomerulus-specific synchronization of mitral cells in the olfactory bulb. Neuron 31:639-651.
Severson KS, Xu D, Van de Loo M, Bai L, Ginty DD, O'Connor DH (2017) Active Touch and Self-Motion Encoding by Merkel Cell-Associated Afferents. Neuron 94:666-+.
Shirasu M, Yoshikawa K, Takai Y, Nakashima A, Takeuchi H, Sakano H, Touhara K (2014) Olfactory Receptor and Neural Pathway Responsible for Highly Selective Sensing of Musk Odors. Neuron 81:165-178.
Shusterman R, Smear MC, Koulakov AA, Rinberg D (2011) Precise olfactory responses tile the sniff cycle. Nature neuroscience 14:1039-1044.
Shusterman R, Sirotin YB, Smear MC, Ahmadian Y, Rinberg D (2018) Sniff Invariant Odor Coding. eNeuro 5.
Smear M, Resulaj A, Zhang J, Bozza T, Rinberg D (2013) Multiple perceptible signals from a single olfactory glomerulus. Nature neuroscience.
Spors H, Grinvald A (2002) Spatio-temporal dynamics of odor representations in the

mammalian olfactory bulb. Neuron 34:301-315.
Stettler DD, Axel R (2009) Representations of odor in the piriform cortex. Neuron 63:854-864.
Storace DA, Cohen LB (2017) Measuring the olfactory bulb input-output transformation reveals a contribution to the perception of odorant concentration invariance. Nature Communications 8.
Uchida N, Mainen ZF (2003) Speed and accuracy of olfactory discrimination in the rat. Nat neurosci 6:1224-1229.
Uchida N, Eshel N, Watabe-Uchida M (2013) Division of Labor for Division: Inhibitory lnterneurons with Different Spatial Landscapes in the Olfactory System. Neuron 80:1106-1109.
Uchida N, Takahashi YK, Tanifuji M, Mori K (2000) Odor maps in the mammalian olfactory bulb: domain organization and odorant structural features. Nature Neuroscience 3:1035-1043.
Vincis R, Lagier S, Van De Ville D, Rodriguez I, Carleton A (2015) Sensory-Evoked Intrinsic Imaging Signals in the Olfactory Bulb Are Independent of Neurovascular Coupling. Cell Rep 12:313-325.
Wachowiak M, Cohen LB (2001) Representation of odorants by receptor neuron input to the mouse olfactory bulb. Neuron 32:723-735.
Wachowiak M, McGann JP, Heyward PM, Shao Z, Puche AC, Shipley MT (2005) Inhibition [corrected] of olfactory receptor neuron input to olfactory bulb glomeruli mediated by suppression of presynaptic calcium influx. J Neurophysiol 94:2700-2712.
Whitesell JD, Sorensen KA, Jarvie BC, Hentges ST, Schoppa NE (2013) Interglomerular lateral inhibition targeted on external tufted cells in the olfactory bulb. Journal of neuroscience 33:1552-1563.
Wilson CD, Serrano GO, Koulakov AA, Rinberg D (2017) A primacy code for odor identity. Nature Communications 8.
Yamada Y, Bhaukaurally K, Madarasz TJ, Pouget A, Rodriguez I, Carleton A (2017) Context- and Output Layer-Dependent Long-Term Ensemble Plasticity in a Sensory Circuit. Neuron 93:1198-+.
Yokoi M, Mori K, Nakanishi S (1995) Refinement of odor molecule tuning by dendrodendritic synaptic inhibition in the olfactory bulb. Proceedings of the National Academy of Sciences of the United States of America 92:3371-3375.
Yoles-Frenkel M, Kahan A, Ben-Shaul Y (2018) Temporal Response Properties of Accessory Olfactory Bulb Neurons: Limitations and Opportunities for

Decoding. Journal of Neuroscience 38:4957-4976.

Further Reading

Chong E, Rinberg D (2018) Behavioral readout of spatio-temporal codes in olfaction. Current Opinion in Neurobiology 52:18-24.

Kepecs A, Uchida N, Mainen ZF (2006) The sniff as a unit of olfactory processing. Chemical Senses 31:167-179.

Mori K, Takahashi YK, Igarashi KM, Yamaguchi M (2006) Maps of odorant molecular features in the Mammalian olfactory bulb. Physiological Reviews 86:409-433.

Uchida N, Poo C, Haddad R (2014) Coding and transformations in the olfactory system. Annual review of neuroscience 37:363-385.

Wilson RI, Mainen ZF (2006) Early events in olfactory processing. Annu Rev Neurosci 29:163-201.

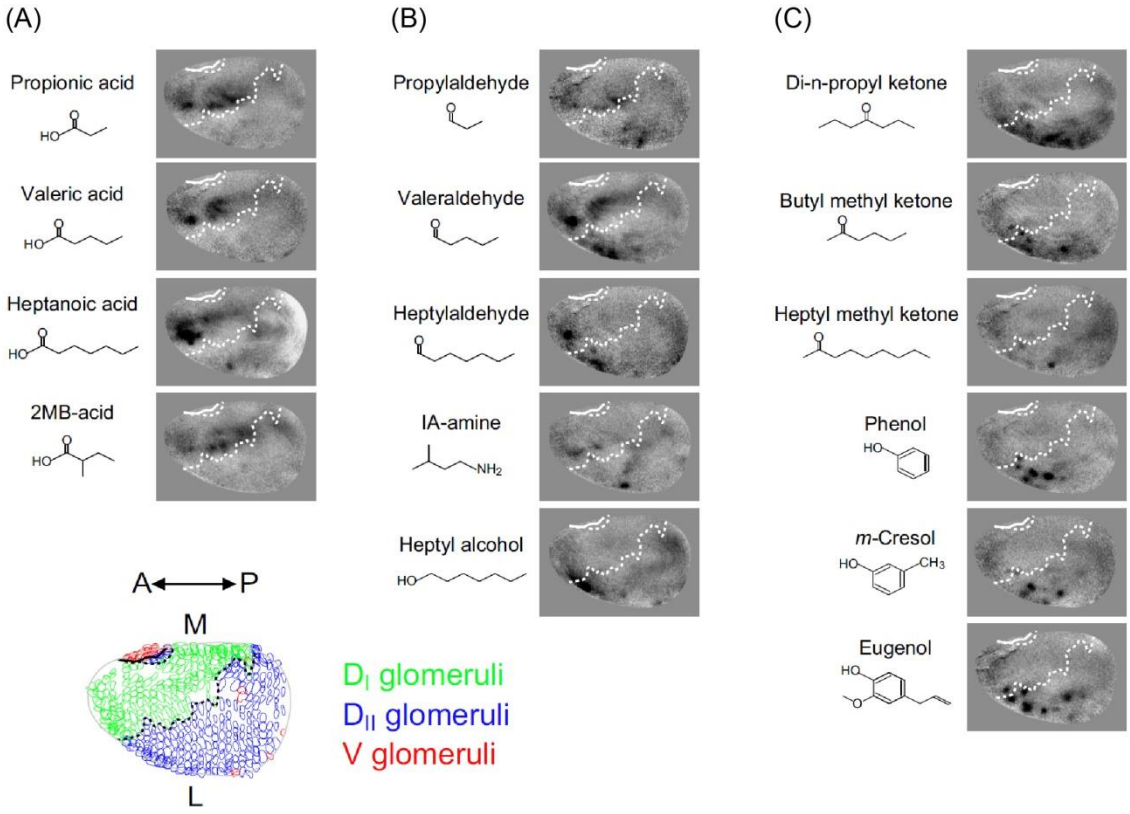

Figure 1

Odor map and domain organization of the OB. Intrinsic signals in the dorsal surface of the OB were analyzed for various odorants. Intrinsic signals represent activity in OSN axons (Vincis et al., 2015). Each odorant typically activates multiple glomeruli. Accordingly, a variety of odorants can be represented as the combination of activated glomeruli, at the level of OSN axon terminals. Aliphatic acids tend to activate D_I (A), whereas ketones and aromatic compounds tend to activate D_{II} (C). There are also odorants that activate both domains (B). Class II-GFP mice were used to distinguish between D_I and D_{II} domains. Adapted from Kobayakawa et al., 2007, Nature, with permission from Springer Nature.

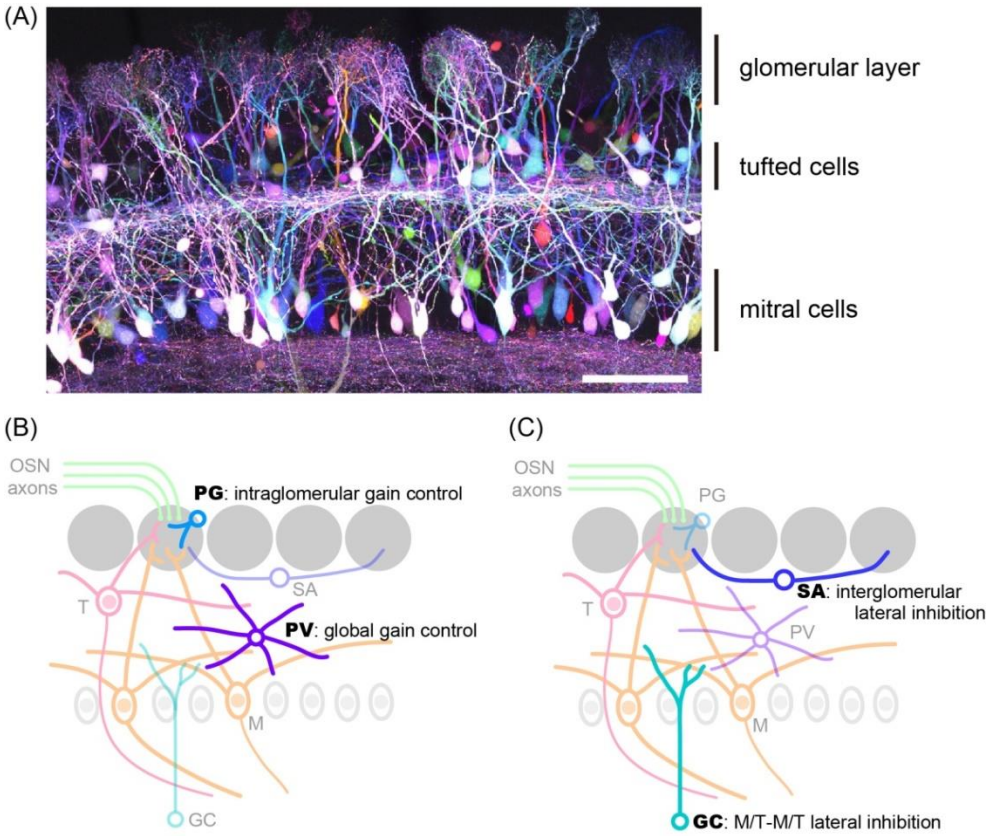

Figure 2

OB circuitry. (A) Mitral and tufted (M/T) cells. M/T cells were labelled with Tetbow allowing for stochastic multicolor labeling (Sakaguchi et al., 2018). Each M/T cell connects a single primary dendrite to a single glomerulus, where they receive both excitatory and inhibitory inputs. M/T cell lateral dendrites and somata receive inputs from inhibitory neurons such as granule cells. These dendrites also release glutamate, forming reciprocal synapses. Each glomerulus is innervated by multiple M/T cells. (B) Gain control mechanisms. Periglomerular interneurons mediate intraglomerular gain control. More global gain control is mediated by parvalbumin-expressing interneurons, and short axon cells. (C) Lateral inhibition in the OB. Interglomerular lateral inhibition is mediated by short axon cells expressing GABA and dopamine. M/T-to-M/T lateral inhibition is mediated by granule cells. M, mitral cells; T, tufted cells; PG, periglomerular cells; SA, short axon cells; PV, parvalbumin-expressing interneurons; GC, granule cells. (A) was modified from Sakaguchi et al., 2018, eLife.

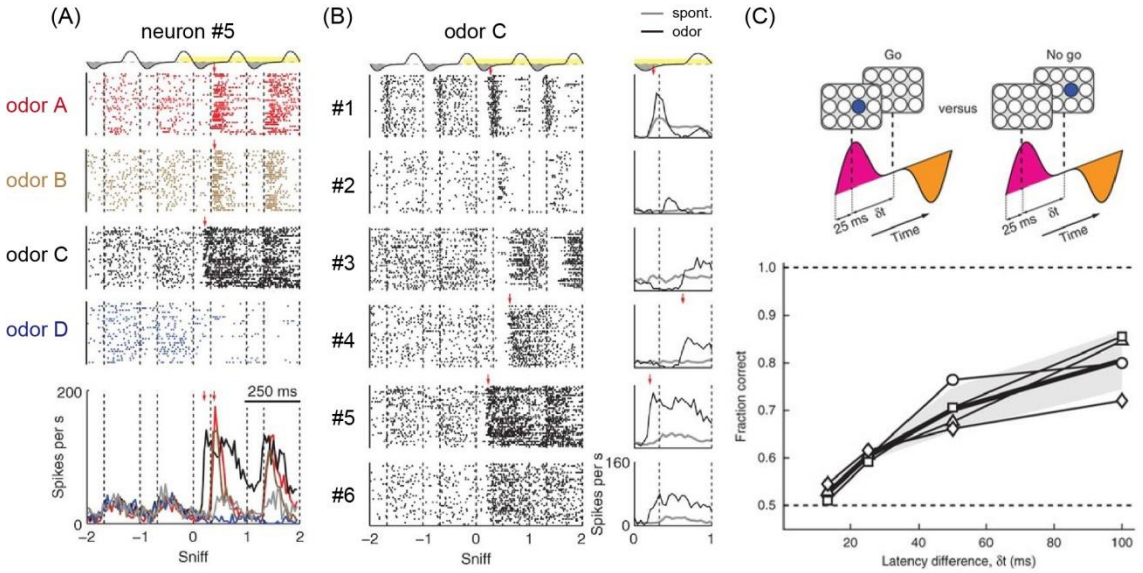

Figure 3

Temporal representation of odors in the OB. (A) One M/T cell's responses to four different odors are shown. Sniff-warped raster plots are shown. Each M/T cell responds to different odors at a different timing (phase) in the sniff cycle. The response phase is reproducible among trials. Peristimulus time histogram plots are shown on the bottom. (B) Responses of six M/T cells to the same odor. Peristimulus time histogram plots are shown on the right. (C) Discrimination of timing differences for a single glomerulus. Mice could discriminate between optogenetic activation of a M71-ChR2 glomerulus early in a sniff cycle from that which occurred at a later timing. Black lines indicate the performance of individual mice. The thick black line and shades indicate mean +/- SD. (A) and (B) are modified from Shusterman et al., 2011, Nat Neurosci, and (C) is adapted from Smear et al., 2013, Nat Neurosci, with permission from Springer Nature.

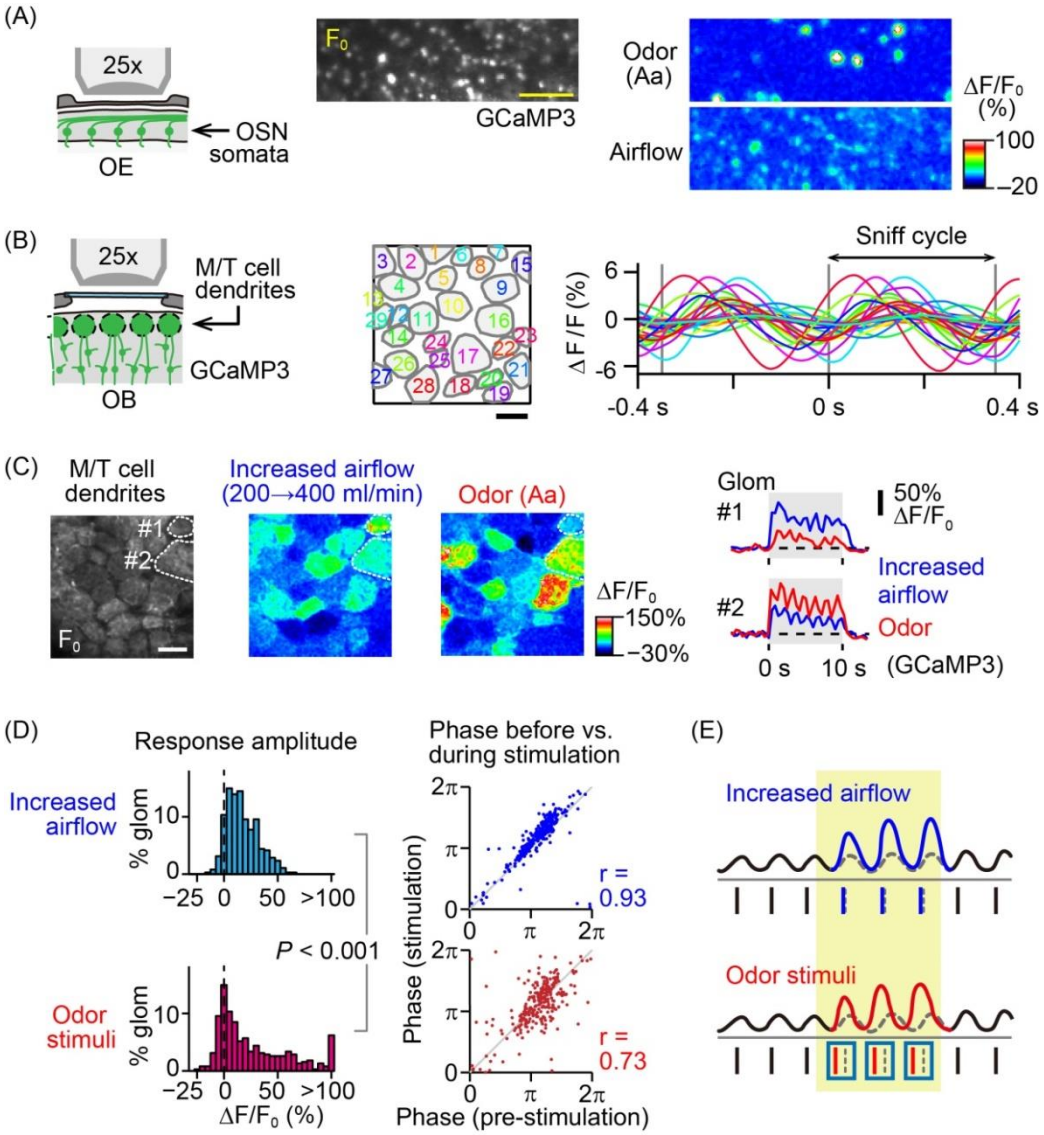

Figure 4

Mechanosensory-based phase coding. (A) Airflow-driven mechanosensation in OSNs visualized by two-photon calcium imaging of the OE. OSN-GCaMP3 mice were analyzed. (B) Mechanosensory-based oscillatory activity in M/T cells. Cycle-averaged traces for glomeruli were determined based on two-photon calcium imaging of a M/T-GCaMP3 mouse. (C) Airflow-driven (increase in airflow speed) and odor-evoked (amyl acetate) responses in M/T cells. Both activate M/T cell responses in terms of rate coding. (D) Phase shifts in the oscillations produced by the increased airflow and odor stimuli. (E) Both airflow and odor stimuli change the rate code, but only the latter produces changes in the phase code. Thus, phase coding can distinguish between odor signals and changes in sniff conditions. Images are modified from Iwata et al., 2017, Neuron.

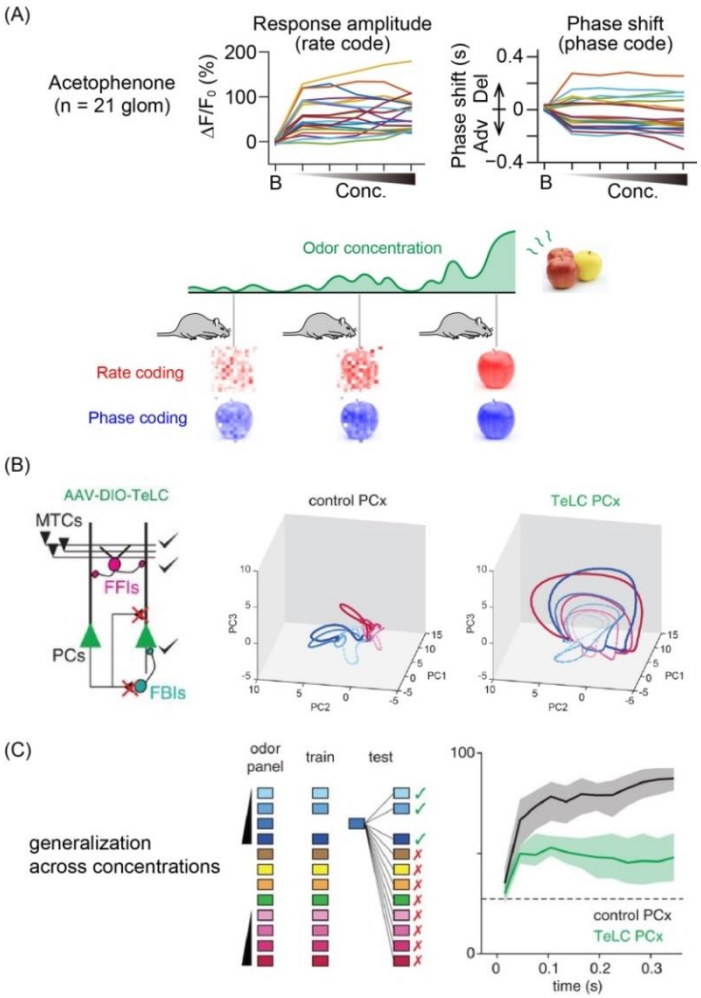

Figure 5

Concentration invariant odor coding. (A) Phase coding in the OB is concentration-invariant, while rate coding is variable across concentrations. Note that not all of the glomeruli show a tonic increase in rate code (□F/F$_0$) as the concentration increases, leading to a rearrangement of the odor map. Phase coding may be useful for odor identity coding, by which animals can track the scent of an odor to the source despite the fluctuations in odor concentrations. (B) Feedback inhibition (FBI) within the piriform cortex (PCx) is required for the concentration-invariant odor representation in the PCx. Expression of tetanus toxin light chain (TeLC) blocks FBI and impairs the concentration-invariant representation in PCx. Odor response trajectories in a PCA space for two odors (red and blue) are shown for different concentrations. (C) Decoding analysis of PCx activity in control and TeLC. A linear decoder was used to classify different odors at variable concentrations. Decoding accuracy was reduced in TeLC PCx. (A) is adapted from Iwata et al., 2017, Neuron. (B) and (C) are adapted from Bolding & Franks, 2018, Science (also published in bioRxiv).

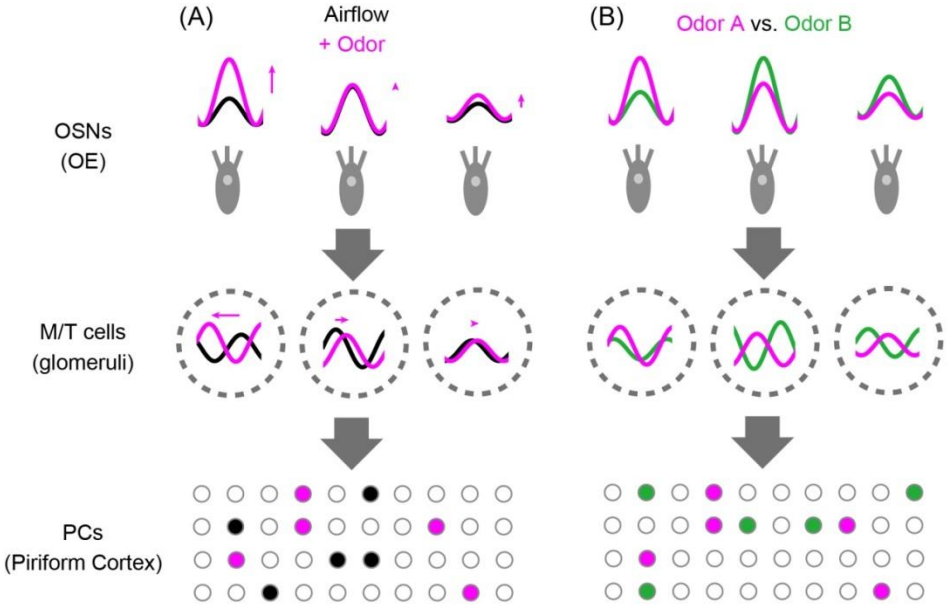

Figure 6

Coding strategy in OSNs, M/T cells, and pyramidal cells (PCs) in the piriform cortex.